Desalination and Water Treatment
www.deswater.com

doi: 10.1080/19443994.2014.927334

55 (2015) 1816–1824
August

Taylor & Francis
Taylor & Francis Group

Optimization of Cu(II), Ni(II), Cd(II) and Pb(II) biosorption by red marine alga *Kappaphycus alvarezii*

R.S. Praveen, K. Vijayaraghavan*

Department of Chemical Engineering, Indian Institute of Technology Madras, Chennai 600036, India, Tel. +91 44 22575156; email: prawinsubay@yahoo.com (R.S. Praveen), Tel. +91 44 22575156; Fax: +91 44 22570509; email: cevijay@iitm.ac.in (K. Vijayaraghavan)

Received 16 December 2013; Accepted 18 May 2014

ABSTRACT

The aim of this investigation was to study the potential of red seaweed *Kappaphycus alvarezii* for the removal of Cu(II), Ni(II), Cd(II) and Pb(II) from aqueous solutions. The mechanism of biosorption was identified as the interaction of positively charged metal ions and negatively charged functional groups on the surface of *K. alvarezii* through FTIR and SEM analysis. Owing to the above mechanism, the biosorption capacity of red seaweed was significantly affected by solution pH. Biosorption isotherms obtained at pH 4.5 indicated that *K. alvarezii* provided higher uptake for Pb (0.51 mmol/g), followed by Cd (0.48 mmol/g), Cu (0.47 mmol/g) and Ni (0.38 mmol/g). The reason for varied affinity of a biosorbent towards a particular metal ion was correlated with its atomic weight, ionic radius and electronegativity. Of the different isotherm models (Langmuir, Freundlich, Toth and Sips), the Toth model better predicted experimental isotherm data with high correlation coefficients and low % error values. Kinetic studies indicated that the rate of metal removal by *K. alvarezii* was high with 90% of the process completed within 45 min. Desorption experiments with different elutants (0.01 M NaOH, 0.1 M NaOH, 0.01 M HCl and 0.1 M HCl) revealed that maximum desorption of all metal ions from metal-loaded *K. alvarezii* can be achieved with 0.01 M HCl.

Keywords: Bioremediation; Biosorption; Heavy metals; Seaweed; Water treatment

1. Introduction

In recent years, industry and government have become increasingly aware of the need to clean-up industrial wastewaters and reduce point-source pollution. Among different pollutants, the presence of heavy metals in wastewater is of serious concern as they are non-biodegradable and cause serious health issues. Many industries, especially plating, painting, leather and mining industries generate large quantities of wastewater containing various concentrations of heavy metals. These wastewaters are to be treated prior to discharge due to the toxicity of heavy metals. The conventional approaches for removing or recovering heavy metals from wastewaters, such as precipitation, oxidation/reduction, activated carbon adsorption, ion-exchange, evaporation and electrochemical processes were identified to possess either of the following constraints, including high cost, incomplete removal, low selectivity, high energy consumption and generation of toxic slurries [1]. Hence, there is an

*Corresponding author.

urgent need to find alternative cheap and efficient technologies to substitute the existing processes for treatment of metal-bearing wastewaters.

Biosorption is an alternative technology to remove heavy metals from wastewaters. The process involves a solid phase (biosorbent with favourable functional groups) and a liquid phase (solvent containing dissolved sorbate species). Due to higher affinity of the sorbent for the sorbate species, the latter is attracted and bound to the sorbent through various mechanisms. The process continues till equilibrium is established between the amount of solid-bound sorbate species and its portion remaining in the solution. Of the different mechanisms, metal sorption by biosorbents occurs via ion-exchange, complexation, coordination, chelation, micro-precipitation and/or combination of these mechanisms [2]. Different biosorbents such as inactive/dead bacteria [3], fungi [4], algae [5], yeast [6] as well as agricultural [7] and industrial [8] wastes have been widely used for the removal of heavy metal ions. The feasibility of using inactive/dead seaweeds as potential biosorbents for heavy metals has been studied widely in recent years [9–11], as the process offers several advantages including low operating cost, continuous availability of biosorbent, high performance and reusability of biosorbent in multiple cycles. In particular, brown seaweeds have been extensively studied for heavy metal ions [12]. However, other types such as red and green seaweeds have been less focussed in biosorption research. Among few biosorption studies using red seaweeds, Hashim and Chu [13] reported that among different seaweed species examined for Cd biosorption, the red seaweed (*Gracilaria salicornia*) exhibited lowest uptake of 0.16 mmol/g. Vijayaraghavan et al. [14] identified that brown seaweeds (*Sargassum wightii* and *Sargassum illcifolium*) outperformed red seaweeds (*Gracilaria edulis* and *Geledium* sp.) in Co(II) and Ni(II) biosorption. The cell wall composition is portrayed as the main reason for poor biosorption potential of red seaweeds [14,15]. In contrast to alginate in brown seaweed, the cell wall of red algae is mainly composed of carrageenans and agar [16]. However, the mediocre biosorption potential was based on only few species of red seaweeds and additional research should be performed to elucidate the potential of other types of red seaweeds.

Therefore, this research focussed on using a new red alga (*Kappaphycus alvarezii*) for the biosorption of Cu(II), Ni(II), Cd(II) and Pb(II) ions. *Kappaphycus* species are among the largest tropical red algae, with a rapid growth rate [17]. Even though the algae has commercial applications, the high growth rate, plastic morphology and extremely successful vegetative regeneration make *Kappaphycus* species a potentially destructive invasive in many parts of world oceans. Thus, an alternative application for *K. alvarezii* is desirable. The present research also provides insights into the binding mechanism responsible for the removal of heavy metal ions by *K. alvarezii* and identifies the major parameters affecting its biosorption.

2. Materials and methods

2.1. Red algae collection and metal solute preparation

Samples of *K. alvarezii* were collected from the Mandapam (9°16′47′′N 79°7′12′′E) region of Tamil Nadu, India. The seaweed biomass was washed with de-ionized (DI) water and then dried under the sun for 2 d. The dried seaweed biomass was then grounded to an average particle size of 0.75 mm.

Stock solutions (10 mmol/L) of Cu(II), Ni(II), Cd(II) and Pb(II) were prepared using $Cu(NO_3)_2{\cdot}3H_2O$, $Ni(NO_3)_2{\cdot}6H_2O$, $Cd(NO_3)_2{\cdot}4H_2O$ and $Pb(NO_3)_2$, respectively. The desired concentrations were obtained by the dilution of stock solution with DI water during the course of experiment.

2.2. Procedure for metal biosorption experiments

All experiments were conducted using 250 mL Erlenmeyer flasks at 32 ± 1°C in an incubated shaker. In each flask, 0.2 g of *K. alvarezii* was amended with 100 mL of one of the four metal ions (Cu(II), Ni(II), Cd (II) and Pb(II)) in appropriate concentration ranges. The contents of the flask were agitated in an incubated rotary shaker at 160 rpm for 4 h. The pH of metal solution was initially adjusted and maintained using 0.1 M HCl or NaOH. After equilibrium, the suspension was filtered using 0.45 μm PTFE membrane filter and the supernatant was analysed for metal concentrations using inductively coupled plasma-optical emission spectrometry (ICP-OES, Perkin Elmer Optima 5300 DV). The pH edge experiments were conducted at different pH conditions (pH 2.5–5) at fixed initial metal concentration of 1 mmol/L. In contrary, isotherm experiments were conducted at optimal pH of 4.5 by varying initial metal concentrations (1–10 mmol/L). Kinetic experiments were conducted at pH 4.5 and initial metal concentration of 1 mmol/L. Samples of 0.1 mL each were drawn from the mixture at pre-determined time intervals to generate kinetics data.

The amount of metal biosorbed by *K. alvarezii* was calculated from the difference between the metal quantity added to the biomass and the metal content of the supernatant using the following equation,

$$q = V(C_0 - C_e)/M \quad (1)$$

where q is the amount of the metal adsorbed (mmol/g), V is the volume of metal solution (L), C_0 and C_e are the initial and equilibrium metal concentrations in the solution (mmol/L), respectively, and M is the mass of biomass (g). After completion of biosorption experiments, the metal-loaded *K. alvarezii* was filtered and exposed subsequently to different elutant solutions in the Erlenmeyer flask. To achieve high concentration factor, only 50 mL of elutant solution was employed. The contents were agitated at 160 rpm for 1 h. After filtration, the metal content in the supernatant was determined using ICP-OES. The desorption efficiency was determined from the ratio of the mass of metal ion in solution after desorption to the mass of metal ion initially bound to the biosorbent.

Isotherm and kinetic model parameters were evaluated by non-linear regression using SigmaPlot (version 4.0, SPSS, Chicago, IL). The average percentage error between the experimental and predicted values is calculated using:

$$\varepsilon\,(\%) = \frac{\sum_{i=1}^{N}\left(q_{\mathrm{exp},i} - q_{\mathrm{cal},i}/q_{\mathrm{exp},i}\right)}{N} \times 100 \quad (2)$$

where q_{exp} and q_{cal} represent experimental and calculated metal uptake values, respectively, and N is the number of measurements.

2.3. Biomass characterization study

The mechanism of metal removal by *K. alvarezii* and the involvement of functional groups were determined using a Bruker-ATR IR (ACPHA) Fourier Transform IR spectrophotometer (Germany). The samples were prepared in the form of pellets using KBr. To understand the algal surface morphology and sorption removal mechanism of *K. alvarezii*, the samples before and after adsorption of metal ions were dried, coated with thin layer of gold and subsequently analysed using scanning electron microscopy (Hitachi S4800, Japan).

3. Results and discussion

3.1. pH edge studies

Solution pH plays a vital role in deciding the maximum biosorption potential of any biosorbent. It affects the surface charge of the sorbent, the degree of ionization and speciation of the surface functional groups and metal ions [18]. Therefore, metal removal as a function of equilibrium pH was studied first and the results are shown in Fig. 1. It was clear that % removal of all metal ions by *K. alvarezii* increases with increase in pH from pH 2.5 to 4.5 and thereafter decreases with further increase in equilibrium pH. This behaviour can be explained on the basis of biomass functional groups and speciation of metal ions at different pH conditions. The cell wall of red seaweed mainly composed of polysaccharides such as carrageenans and agar. Carrageenan consists of alternating 3-linked-β-D-galactopyranose units, while the gelling hydrocolloid agar is mainly comprised of L-rather than D-3,6-anhydro-α-galactopyranose units [16]. Among different functional groups, carboxyl and sulphonate groups are prevalent [19] in polysaccharides of red seaweed. At low pH (acidic) values, these negatively charged functional groups are protonated with H^+ ions and hence may not able to accommodate positively charged target metal ions (Cu^{2+}, Ni^{2+}, Cd^{2+} and Pb^{2+}). As the pH increases, the concentration of H^+ ions decreases and positively charged target metal ions can interact with the negatively charged binding sites of *K. alvarezii*. The speciation of heavy metal ions is also strongly influenced by pH. At acidic pH values (pH ≤ 5), all the examined heavy metal ions exists in their divalent form. At pH values greater than 5, precipitation occurs for some heavy metal ions such as lead and thus experiments were not conducted beyond pH 5.

Analysing the results of Fig. 1, it can inferred that *K. alvarezii* biosorbed more Pb^{2+}, followed by Cd^{2+}, Cu^{2+} and Ni^{2+}. The affinity of a biosorbent towards a particular metal ion can be correlated with its atomic weight, ionic radius and electronegativity [20]. The atomic weight is in the order of Pb (207.2) > Cd (112.4) > Cu (63.5) > Ni (58.7). In contrary, electronegativity decreases in the order of Pb (2.33) > Ni (1.91) > Cu (1.9)

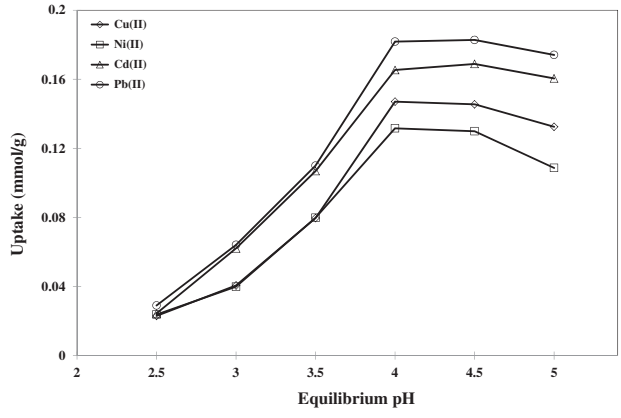

Fig. 1. Influence of equilibrium pH on metal uptake capacity of *K. alvarezii* (temperature = 32 ± 1 °C).

> Cd (1.69). In the case of ionic radii, Pb (133) > Cd (109) > Cu (87) > Ni (83). The experimental uptakes at optimum pH 4.5 were in the order of Pb (0.18 mmol/g) > Cd (0.17 mmol/g) > Cu (0.15 mmol/g) > Ni (0.13 mmol/g). Thus, a clear correlation was obtained between the extent of metal ions biosorbed and properties of metals (atomic weight and ionic radii). Even though electronegativity of Cd found to be least compared to other metals examined, the atomic weight and ionic radii favoured Cd to be biosorbed more than Cu and Ni.

3.2. *Characterization of* K. alvarezii

FTIR spectroscopy analysis has widely been used in sorption studies to detect vibrational frequency changes in sorbent and allows identification of functional groups responsible for the removal of metal ions. In the present study, the assignment of FTIR spectroscopy peaks to the specific functional groups is based on previous reports [21,22]. Seaweeds have been evaluated to be comprised of several chemical groups including carboxyl, amino, sulphonate, and hydroxyl. Fig. 2 illustrates the FTIR spectra of virgin seaweed along with metal-loaded *K. alvarezii*. It was obvious that virgin *K. alvarezii* displayed a number of absorption peaks, indicating the complex nature of the biosorbent. The virgin seaweed displayed peaks at 3,368 cm^{-1} (–OH, –NH stretching), 1,634 cm^{-1} (asymmetric C=O stretch of COOH), 1,424 cm^{-1} (symmetric C=O), 1,377 cm^{-1} (asymmetric $–OSO_3$), 1,215 cm^{-1} (C–O (COOH) stretch), 1,134 cm^{-1} (symmetric $–OSO_3$) and 1,024 cm^{-1} (C–O (alcohol) band). Significant changes in biomass functionalities were visible after exposure to metal ions (Fig. 2). This is due to the displacement of natural ionic species on the biomass surface by the metal ions of interest which causes changes to the observed wave numbers. Biomass carboxyl played a major role in metal binding as shown by changes in peak wave numbers. In particular, major shifts were observed with asymmetric and symmetric C=O and C–O stretches in metal-loaded samples of *K. alvarezii* compared to virgin *K. alvarezii* (Table 1). Similarly, involvement of sulphonate groups was also confirmed as significant shifts were identified with symmetric and asymmetric $–OSO_3$ bands in comparison with virgin *K. alvarezii* (Table 1). The results confirmed the involvement of acidic functional groups (carboxyl and sulphonate) in binding of heavy metal ions.

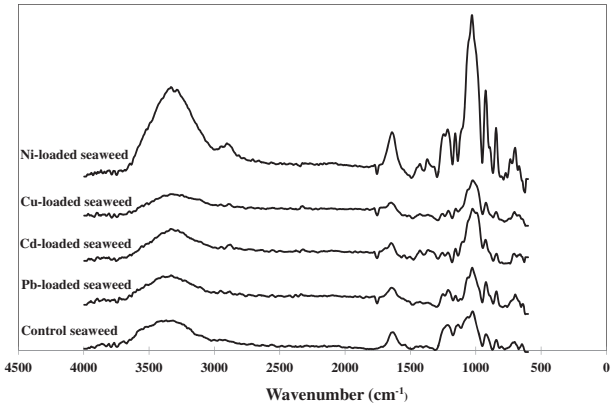

Fig. 2. FTIR spectra of virgin and metal-loaded *K. alvarezii*.

Fig. 3 shows the SEM images of virgin and Pb-loaded *K. alvarezii*. The surface of virgin *K. alvarezii* was found to comprise protuberances and microstructures, which may be due to sodium and other salt crystalloid deposition [23]. After biosorption, the surface of *K. alvarezii* appeared flat in comparison to the virgin seaweed sample for all metal ions examined. The samples were also exposed to EDX analysis (Fig. 3). In virgin seaweed sample, strong Na and K peaks were observed. These ions were acquired by *K. alvarezii* from seawater. In Pb-loaded *K. alvarezii* sample, strong peaks of Pb were observed. Also from Fig. 3(b), it is interesting to note that Na peaks disappeared and the intensity of K peaks decreased when compared to virgin seaweed sample, indicating that ion-exchange is the mechanism of metal removal in which light metal ions were exchanged with metal ion of interest during biosorption. Similar results were obtained for other metal ions (Figures not presented).

3.3. *Time course of metal uptake by* K. alvarezii

Fig. 4 shows the biosorption kinetics for Cu, Ni, Cd and Pb. Biomass of *K. alvarezii* enabled rapid removal of all examined metal ions under the experimental conditions. Within 45 min, 90% of total removal was achieved by *K. alvarezii* for all metal ions. This initial rapid phase was followed by relatively slow phase which eventually resulted in attainment of equilibrium, as evidenced by a plateau, at 120 min. Consequently, a contact time of 4 h was chosen for establishing the biosorption isotherms. The initial quick phase (up to 45 min) can be attributed to the presence of excessive vacant binding sites for biosorption during early stages, which can be occupied by metal ions. As the time progresses, the occupation of remaining vacant sites would be difficult because of the repulsive forces between the solute molecules on the solid and bulk phases [24]. On comparing the rates at which *K. alvarezii* biosorbed four metal ions, no significant differences were observed (Fig. 4). Nevertheless, the quantities of metals sorbed were different for each metal ion.

Table 1
Stretching frequencies observed in virgin and metal-loaded *K. alvarezii* [21,22]

Assignment	Wave number (cm^{-1})				
	Control seaweed	Pb-loaded seaweed	Cd-loaded seaweed	Cu-loaded seaweed	Ni-loaded seaweed
–OH, –NH stretching	3,368	3,331	3,335	3,327	3,331
Asymmetric C=O stretch of COOH	1,634	1,646	1,646	1,648	1,640
Symmetric C=O	1,424	1,428	1,428	1,428	1,426
Asymmetric $–OSO_3$	1,377	1,362	1,362	1,362	1,370
C–O (COOH) stretch	1,215	1,211	1,211	1,209	1,213
Symmetric $–OSO_3$	1,134	1,154	1,154	1,150	1,156
C–O (alcohol) band	1,024	1,026	1,026	1,022	1,028

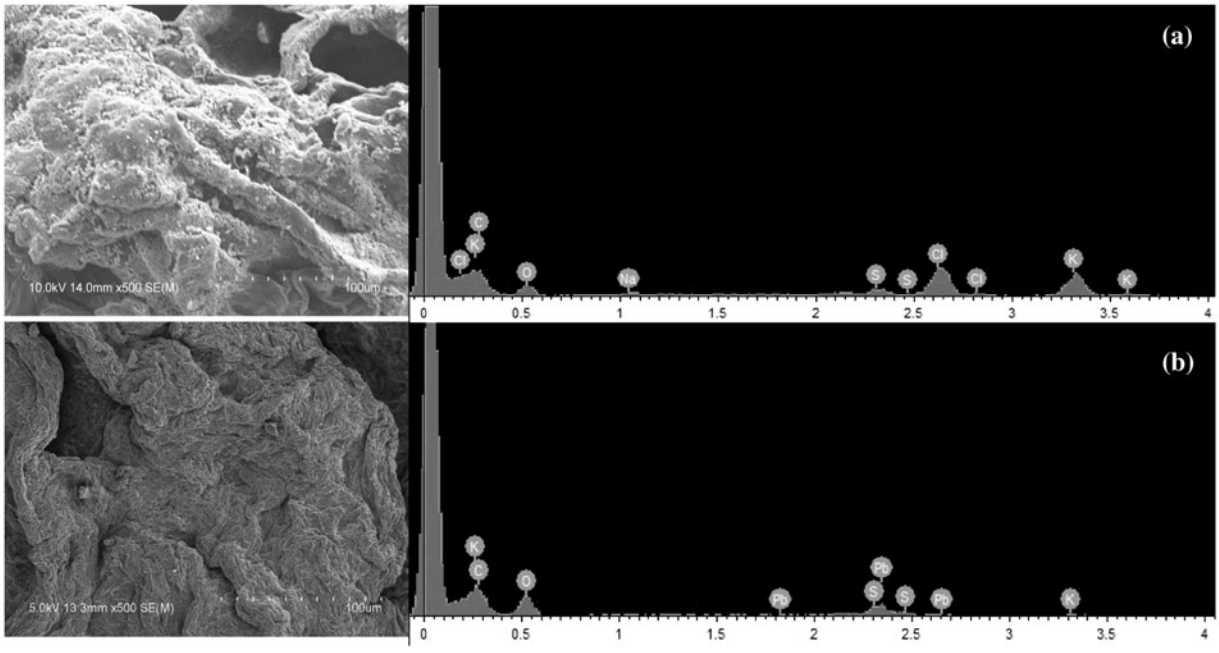

Fig. 3. SEM and EDX images of (a) virgin *K. alvarezii* and (b) Pb-loaded *K. alvarezii*.

In an effort to evaluate the kinetics of metal uptake and the differences in the biosorption kinetic rates, the experimental data were modelled using the Elovich, pseudo-first- and second-order models. The models are represented as follows,

$$\text{Elovich model: } q_t = \frac{1}{b}\ln(1+abt) \quad (3)$$

$$\text{Pseudo-first-order model: } q_t = q_e(1-\exp(-k_1 t)) \quad (4)$$

$$\text{Pseudo-second-order model: } q_t = \frac{q_e^2 k_2 t}{1+q_e k_2 t} \quad (5)$$

where a is the initial adsorption rate (mmol/(g.min)), b is the desorption constant (g/mmol), q_t is the amount of metal sorbed at time t (mmol/g), q_e is the amount of metal sorbed at equilibrium (mmol/g), k_1 is the pseudo-first-order rate constant (min^{-1}) and k_2 is the pseudo-second-order rate constant (g/mmol.min). The model constants along with correlation coefficient (R^2) and % error (ε) values are presented in Table 2. The Elovich equation describes chemical adsorption on heterogeneous surfaces, however, does not propose any definite mechanism for sorbate–sorbent interaction [25]. The equation is commonly used to describe the sorption behaviour with a rapid equilibrium rate in the early period, while it slows down the equilibrium

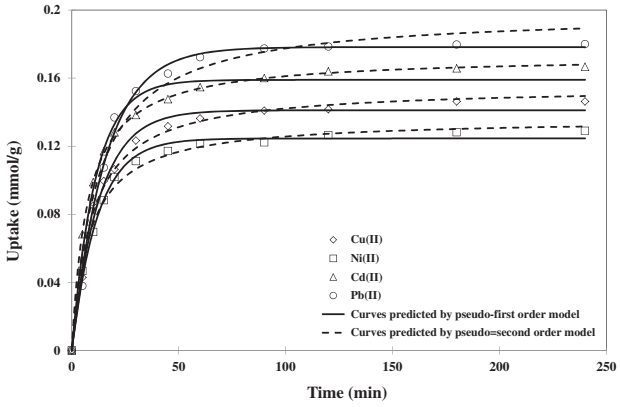

Fig. 4. Biosorption kinetics of *K. alvarezii* towards different metal ions (pH 4.5; temperature = 32 ± 1 °C).

at later periods of the sorption process. The constants "a" and "b" represent the rate of sorption and surface coverage, respectively. The predication of experimental kinetic data were not satisfactory especially during later stages ($t > 45$ min) (Figure not presented) and this trend resulted in low R^2 and high ε values (Table 2). On the other hand, the pseudo-first-order model showed better agreement with the experimental kinetic data with very high R^2 and low ε values (Table 2). The predicted q_e values followed the sequence: Pb > Cd > Cu > Ni. However, on testing the validity of the pseudo-first-order model, it turns out that q_e values obtained from the model underpredicted the experimental q_e values of 0.18, 0.17, 0.15 and 0.13 mmol/g for Pb, Cd, Cu and Ni, respectively. The reason for these differences in prediction was due to a

Table 2
Isotherm and kinetic model constants obtained during metal biosorption onto *K. alvarezii*

		Cu(II)	Ni(II)	Cd(II)	Pb(II)
Langmuir	q_{max} (mmol/g)	0.47	0.38	0.48	0.51
	b_L (L/mmol)	0.636	0.786	0.886	0.949
	R^2	0.998	0.998	0.997	0.997
	% error	0.16	0.42	0.43	0.41
Freundlich	K_F (mmol/g) (L/mmol)$^{1/n_F}$	0.20	0.18	0.24	0.26
	n_F	2.98	3.44	3.57	3.64
	R^2	0.978	0.970	0.966	0.966
	% error	1.54	1.75	1.83	1.82
Toth	q_{max} (mmol/g)	0.45	0.35	0.45	0.47
	b_T (L/mmol)	0.62	0.64	0.72	0.77
	n_T	0.96	0.74	0.76	0.75
	R^2	0.998	0.999	0.998	0.999
	% error	0.10	0.02	0.04	0.01
Sips	K_S (L/g) β_S	0.30	0.30	0.42	0.48
	a_S (L/mmol) β_S	0.63	0.78	0.88	0.94
	β_S	0.94	0.92	0.96	0.98
	R^2	0.998	0.997	0.996	0.997
	% error	0.32	0.48	0.47	0.44
Elovich	a (mmol/(g min))	0.075	0.090	0.16	0.050
	b (g/mmol)	41.1	49.3	40.8	28.7
	R^2	0.941	0.944	0.967	0.915
	% error	3.25	2.08	1.14	6.76
Pseudo-first-order	q_e (mmol/g)	0.14	0.12	0.16	0.18
	k_1 (min^{-1})	0.078	0.0831	0.0908	0.0636
	R^2	0.9905	0.9945	0.9827	0.994
	% error	0.11	0.53	0.98	2.01
Pseudo-second-order	q_e (mmol/g)	0.16	0.14	0.17	0.20
	k_2 (g/(mmol min))	0.70	0.88	0.78	0.42
	R^2	0.991	0.993	0.999	0.977
	% error	1.67	0.73	0.14	4.36

time lag, possibly resulting from a boundary layer or an external resistance controlling the initial stage of sorption process [26]. Conversely, the pseudo-second-order model overpredicted the experimental q_e values (Table 2). Several studies reported that the pseudo-second-order model tends to overpredict q_e values [27,28]. Fig. 4 shows the kinetic curves as predicted by pseudo-first- and -second-order models in comparison with experimental kinetic data.

3.4. Biosorption isotherms

Fig. 5 shows the equilibrium biosorption isotherms of Pb, Cd, Cu and Ni by *K. alvarezii*. Sorption isotherms are important to determine the full saturation capacity of any sorbent and it is the plot of sorption uptake (q) vs. the equilibrium metal concentration (C_e) in the solution. In the present study, biosorption isotherms were developed by changing initial metal concentrations in the range of 1–10 mmol/L at pH 4.5. In general, the isotherm rises sharply in the initial stages and reached plateau at higher initial metal concentrations. The steep increase in the initial stages is due to the availability of readily accessible sites which were plenty compared to the moles of metal ions. As the concentration of metal ions increases, the ratio of binding sites to moles of metal ions decreases which leads to a plateau. From Fig. 5, it was observed that favourable L-shaped isotherm was obtained for all four metal ions. Comparing the isotherms, it was clear that isotherm obtained for Pb exhibited steep slope followed by Cd, Cu and Ni. Also, the experimental uptakes were in the order of Pb (0.45 mmol/g) > Cd (0.42 mmol/g) > Cu (0.40 mmol/g) > Ni (0.33 mmol/g).

The experimental isotherms were correlated using two-parameter and three-parameter models as follows,

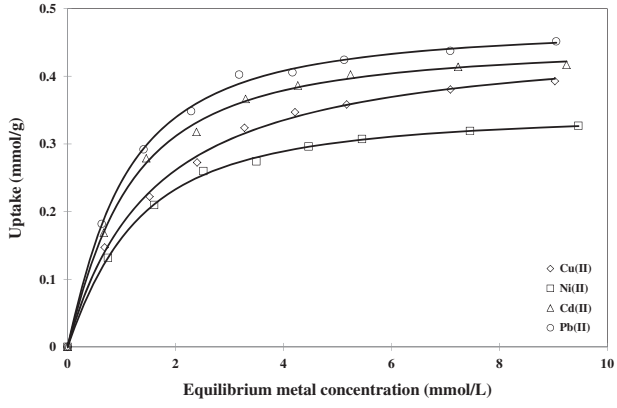

Fig. 5. Biosorption isotherms of different metal ions at pH 4.5 (temperature = 32 ± 1 ℃). Curves were predicted by the Toth model.

$$\text{Langmuir model: } q = \frac{q_{\max} b_L C_e}{1 + b_L C_e} \quad (6)$$

$$\text{Freundlich model: } q = K_F C_e^{1/n_F} \quad (7)$$

$$\text{Sips model: } q = \frac{K_S C_e^{\beta_S}}{1 + a_S C_e^{\beta_S}} \quad (8)$$

$$\text{Toth model: } q = \frac{q_{\max} b_T C_e}{[1 + (b_T C_e)^{1/n_T}]^{n_T}} \quad (9)$$

where q_m is the maximum metal uptake (mmol/g), b_L is the Langmuir equilibrium constant (L/mmol), K_F is the Freundlich constant (mmol/g) $(\text{L/mmol})^{1/n}{}_F$, n_F is the Freundlich exponent, K_S is the Sips model isotherm constant (L/g) β_S, a_S is the Sips model constant (L/mmol) β_S; β_S is the Sips model exponent, b_T is the Toth model constant (L/mmol) and n_T is the Toth model exponent. These models were selected for their simplicity and easily interpretable constants. The model constants are presented in Table 2. At first, the experimental isotherm data were described using the Langmuir model. The model was able to describe the isotherm data with high correlation coefficient ($R^2 > 0.997$) and low % error ($\varepsilon < 0.43\%$) values. The Langmuir model was originally developed for gas absorption but later adopted for biosorption with good success [3]. The model assumes all adsorption sites to be identical, each site retains one molecule and all sites are energetically independent of the adsorbed quantity [29]. In addition, the Langmuir model able to predict the maximum biosorption capacity of any biomass which may not be achievable during experiments. The model constants "$q_{\max}$" correspond to maximum achievable uptake by the biosorbent, and "b_L" is related to the affinity between the sorbate and biosorbent. As shown in Table 2, the *K. alvarezii* exhibited high $q_{\max}$ value for Pb, followed by Cd, Cu and Ni. This sequence was followed according to the ionic radii of metals. In other words, the affinity of metal ions towards the sorbent increases as the size of the metal decreases.

Data prediction by the Freundlich model was significantly inferior to that of Langmuir model (Table 2). Since the Freundlich isotherm equation is exponential, it can only be reasonably applied in the low to intermediate concentration ranges [30]. The model was originally empirical in nature, but was later interpreted to heterogeneous surfaces or surfaces supporting sites of varied affinities. Both the Freundlich isotherm constant (K_F) and exponent (n_F) were recorded high for Pb, followed by other metal ions (Table 2).

In an effort to further enhance the prediction, three-parameter models were used in the present study. The Sips model is a combined form of the Freundlich and Langmuir isotherm equations developed for predicting the heterogeneous adsorption systems. At low solute concentrations, it reduces to Freundlich model; while at high concentrations, it predicts the Langmuir model [31]. The usage of the Sips model to the experimental isotherm data resulted in good prediction ($R^2 > 0.996$ and $\varepsilon < 0.48\%$). Among four metal ions, the Sips isotherm model constant (K_S) recorded high for Pb, followed by Cd, Ni and Cu. The Sips model exponent (β_S) lies close to unity (Table 2), which means that isotherm data were more of the Langmuir form than that of the Freundlich model. The Toth model assumes an asymmetrical quasi-Gaussian energy distribution with most of sites having adsorption energy lower than the maximum or mean values [32]. Similar to other models, magnitude of the Toth model isotherm constant was recorded high for Pb followed by other metal ions. On the basis of R^2 and ε values, the Toth model better described the metal biosorption isotherm data and the predicted curves are illustrated in Fig. 5.

3.5. Desorption

For any successful biosorption process, reuse of biomass is necessary as it will decrease the process cost as well as dependency of the process on continuous supply of biosorbent. A successful desorption process requires the proper selection of eluting agent, which strongly depends on the type of biosorbent and the mechanism of biosorption [33]. Considering that ion exchange is the major mechanism responsible for biosorption by *K. alvarezii* and maximum biosorption occurred in mild acidic conditions (Fig. 1), two elutants including HCl (0.01 and 0.1 M) and NaOH (0.01 and 0.1 M) were examined. Results revealed that both 0.01 and 0.1 M NaOH solutions were not able to desorb metal ions from *K. alvarezii*, as low elution efficiencies were observed for all metal ions (Fig. 6). In contrary, exposure of metal-loaded *K. alvarezii* to HCl resulted in high elution efficiencies. This high performance also confirms the postulated ion-exchange mechanism for the biosorption process as the H^+ ions supplied by the desorbent were exchanged with bounded metal ions in the negatively charged functional groups. Comparing the results based on different strengths of HCl used (Fig. 6), almost identical elution efficiencies were observed for both 0.01 and 0.1 M HCl for all metal ions examined. This implies that 0.01 M can be effectively employed for regeneration of *K. alvarezii* for further usage in biosorption process.

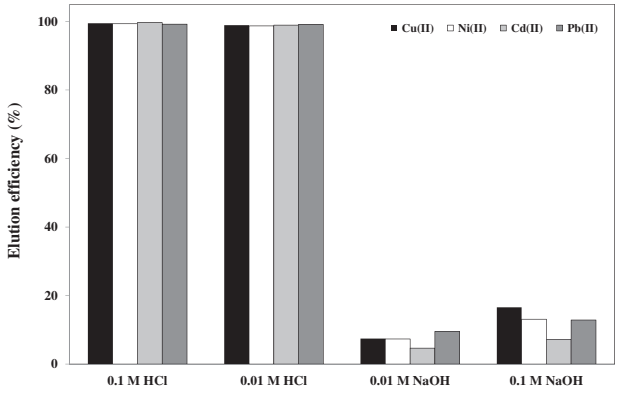

Fig. 6. Desorption performance of different elutants towards metal-loaded *K. alvarezii* (temperature = 32 ± 1 °C).

4. Concluding remarks

Following remarks can be made from the present study,

- In an effort to identify new biosorbent, we report the red seaweed *K. alvarezii* as an efficient sorbent for removal of Cu(II), Ni(II), Cd(II) and Pb(II) ions.
- The experimental results revealed that solution pH strongly influenced biosorption capacity of *K. alvarezii* with pH 4.5 as an optimum for maximum removal of metal ions.
- The mechanism of metal removal was confirmed through SEM and FTIR analysis. The isotherm experiments revealed that *K. alvarezii* possess higher affinity towards Pb(II) ions with an uptake of 0.51 mmol/g, followed by Cd (0.48 mmol/g), Cu (0.47 mmol/g) and Ni (0.38 mmol/g).
- For all metal ions, the biosorption kinetics was found to be rapid with equilibrium attained within 45 min.
- The biosorbed metal ions onto *K. alvarezii* were efficiently desorbed using 0.01 M HCl with elution efficiencies greater than 98.7%. Thus, easy availability, high biosorption capacity, rapid removal rate and easy desorption portray this seaweed-based treatment process as an attractive and viable technique for decontamination of Cu(II), Ni(II), Cd (II) and Pb(II)-bearing wastewaters.

Acknowledgements

This work was financially supported by Ramalingaswami Re-entry Fellowship (Department of Biotechnology, Ministry of India, India) and Fast Track Scheme for Young Scientist (Department of Science and Technology, Ministry of India, India).

References

[1] D. Sud, G. Mahajan, M.P. Kaur, Agricultural waste material as potential adsorbent for sequestering heavy metal ions from aqueous solution—A review, Bioresour. Technol. 99 (2008) 6017–6027.

[2] P. Sar, S.K. Kazy, R.K. Asthana, S.P. Singh, Metal adsorption and desorption by lyophilized *Pseudomonas aeruginosa*, Int. Biodeterior. Biodegrad. 44 (1999) 101–110.

[3] K. Vijayaraghavan, Y.-S. Yun, Bacterial biosorbents and biosorption, Biotechnol. Adv. 26 (2008) 266–291.

[4] R. Dhankhar, A. Hooda, Fungal biosorption—An alternative to meet the challenges of heavy metal pollution in aqueous solutions, Environ. Technol. 32 (2011) 467–491.

[5] E. Romera, F. González, A. Ballester, M.L. Blázquez, J.A. Muñoz, Biosorption with algae: A statistical review, Crit. Rev. Biotechnol. 26 (2006) 223–235.

[6] V. Padmavathy, P. Vasudevan, S.C. Dhingra, Biosorption of nickel(II) ions on Baker's yeast, Proc. Biochem. 38 (2003) 1389–1395.

[7] A. Demirbas, Heavy metal adsorption onto agro-based waste materials: A review, J. Hazard. Mater. 157 (2008) 220–229.

[8] A. Hammaini, F. González, A. Ballester, M.L. Blázquez, J.A. Muñoz, Biosorption of heavy metals by activated sludge and their desorption characteristics, J. Environ. Manage. 84 (2007) 419–426.

[9] V. Murphy, H. Hughes, P. McLoughlin, Comparative study of chromium biosorption by red, green and brown seaweed biomass, Chemosphere 70 (2008) 1128–1134.

[10] N. Koutahzadeh, E. Daneshvar, M. Kousha, M.S. Sohrabi, A. Bhatnagar, Biosorption of hexavalent chromium from aqueous solution by six brown macroalgae, Desalin. Water Treat. 51 (2013) 6021–6030.

[11] K. Vijayaraghavan, U.M. Joshi, Hybrid *Sargassum*-sand sorbent: A novel adsorbent in packed column to treat metal-bearing wastewaters from inductively coupled plasma-optical emission spectrometry, J. Environ. Sci. Health A 48 (2013) 1685–1693.

[12] T.A. Davis, B. Volesky, A. Mucci, A review of the biochemistry of heavy metal biosorption by brown algae, Water Res. 37 (2003) 4311–4330.

[13] M.A. Hashim, K.H. Chu, Biosorption of cadmium by brown, green, and red seaweeds, Chem. Eng. J. 97 (2004) 249–255.

[14] K. Vijayaraghavan, J. Jegan, K. Palanivelu, M. Velan, Biosorption of cobalt(II) and nickel(II) by seaweeds: Batch and column studies, Sep. Purif. Technol. 44 (2005) 53–59.

[15] R.H.S.F. Vieira, B. Volesky, Biosorption: A solution to pollution, Int. Microbiol. 3 (2000) 17–24.

[16] R. Herrero, P. Lodeiro, R. Rojo, A. Ciorba, P. Rodríguez, M.E.S. Sastre de Vicente, The efficiency of the red alga *Mastocarpus stellatus* for remediation of cadmium pollution, Bioresour. Technol. 99 (2008) 4138–4146.

[17] J. Muñoz, Y. Freile-Pelegrín, D. Robledo, Mariculture of *Kappaphycus alvarezii* (Rhodophyta, Solieriaceae) color strains in tropical waters of Yucatán, México, Aquaculture 239 (2004) 161–177.

[18] Z. Reddad, C. Gerente, Y. Andres, P. Le Cloirec, Adsorption of several metal ions onto a low-cost biosorbent: Kinetic and equilibrium studies, Environ. Sci. Technol. 36 (2002) 2067–2073.

[19] M. Sadeghi, Synthesis of a biocopolymer carrageenan-g-poly (AAm-co-IA)/montmorilonite superabsorbent hydrogel composite, Braz. J. Chem. Eng. 29 (2012) 295–305.

[20] I.A. Şengil, M. Özacar, Competitive biosorption of Pb^{2+}, Cu^{2+} and Zn^{2+} ions from aqueous solutions onto valonia tannin resin, J. Hazard. Mater. 166 (2009) 1488–1494.

[21] A.E. Navarro, R.F. Portales, M.R. Sun-Kou, B.P. Llanos, Effect of pH on phenol biosorption by marine seaweeds, J. Hazard. Mater. 156 (2008) 405–411.

[22] V. Murphy, H. Hughes, P. McLoughlin, Enhancement strategies for Cu(II), Cr(III) and Cr(VI) remediation by a variety of seaweed species, J. Hazard. Mater. 166 (2009) 318–326.

[23] K. Vijayaraghavan, M. Sathishkumar, R. Balasubramanian, Interaction of rare earth elements with a brown marine alga in multi-component solutions, Desalination 265 (2011) 54–59.

[24] K. Vijayaraghavan, R. Balasubramanian, Antimonite removal using marine algal species, Ind. Eng. Chem. Res. 50 (2011) 9864–9869.

[25] Y.S. Ho, G. McKay, A comparison of chemisorption kinetic models applied to pollutant removal on various sorbents, Trans. Inst. Chem. Eng. 76B (1998) 332–340.

[26] G. McKay, Y.S. Ho, J.C.P. Ng, Biosorption of copper from waste waters: A review, Sep. Purif. Methods 28 (1999) 87–125.

[27] A.E. Ofomaja, E.B. Naidoo, S.J. Modise, Dynamic studies and pseudo-second order modeling of copper(II) biosorption onto pine cone powder, Desalination 251 (2010) 112–122.

[28] K. Vijayaraghavan, S. Gupta, U.M. Joshi, Comparative assessment of Al(III) and Cd(II) biosorption onto *Turbinaria conoides* in single and binary systems, Water Air Soil Pollut. 223 (2012) 2923–2931.

[29] G. Limousin, J.P. Gaudet, L. Charlet, S. Szenknect, V. Barthès, M. Krimissa, Sorption isotherms: A review on physical bases, modeling and measurement, Appl. Geochem. 22 (2007) 249–275.

[30] Y. Liu, Y.-J. Liu, Biosorption isotherms, kinetics and thermodynamics, Sep. Purif. Technol. 61 (2008) 229–242.

[31] M. Sathishkumar, A.R. Binupriya, K. Vijayaraghavan, S.I. Yun, Two and three-parameter isothermal modelling for liquid-phase sorption of Procion blue H-B by inactive mycelial biomass of *Panus fulvus*, J. Chem. Technol. Biotechnol. 82 (2007) 389–398.

[32] Y.S. Ho, J.F. Porter, G. McKay, Equilibrium isotherm studies for the sorption of divalent metal ions onto peat: Copper, nickel and lead single component systems, Water Air Soil Pollut. 141 (2002) 1–33.

[33] K. Vijayaraghavan, H.Y.N. Winnie, R. Balasubramanian, Biosorption characteristics of crab shell particles for the removal of manganese(II) and zinc(II) from aqueous solutions, Desalination 266 (2011) 195–200.